

Laser Chimeras as a paradigm for multi-stable patterns in complex systems

Laurent Larger[†], Bogdan Penkovsky[†], Yuri Maistrenko[‡]

[†]FEMTO-ST / Optics Dept., UMR CNRS 6174, University of Franche-Comté,
15 avenue des Montboucons, 25030 Besançon Cedex, France and

[‡] Institute of Mathematics and Center for Medical and Biotechnical Research,
NAS of Ukraine, Tereshchenkivska Str. 3, 01601 Kyiv, Ukraine

(Dated: September 13, 2018)

Chimera is a rich and fascinating class of self-organized solutions developed in high dimensional networks having non-local and symmetry breaking coupling features. Its accurate understanding is expected to bring important insight in many phenomena observed in complex spatio-temporal dynamics, from living systems, brain operation principles, and even turbulence in hydrodynamics. In this article we report on a powerful and highly controllable experiment based on optoelectronic delayed feedback applied to a wavelength tunable semiconductor laser, with which a wide variety of Chimera patterns can be accurately investigated and interpreted. We uncover a cascade of higher order Chimeras as a pattern transition from N to $N - 1$ clusters of chaoticity. Finally, we follow visually, as the gain increases, how Chimera is gradually destroyed on the way to apparent turbulence-like system behaviour.

PARADIGM FOR COMPLEXITY: SPACE-TIME VS. TIME DELAY?

Complexity usually develops in high dimensional systems involving nonlinear interactions between system variables. Straightforward paradigmatic experiments to explore and to understand complexity, are generally thought as spatio-temporal nonlinear dynamics with obvious infinite number of degrees of freedom. Such systems provide solutions in high- or infinite dimensional phase space, which degree of complexity depends on the strength of nonlinear effects, as well as on the distribution of coupling between the phase space coordinates (network nodes). The equations of motion appear as a mathematical translation of the deterministic origin ruling the dynamics, e.g. Navier-Stokes equations in fluid dynamics, Ginzburg-Landau equation from superconducting phase transition, reaction-diffusion systems of biological relevance, nonlinear Schrödinger equation in nonlinear optics, and so on. These generic models come however with difficult theoretical analysis as they are essentially nonlinear, and many unsolved hard problems still remain.

Understanding the rules governing complexity remains a Human challenge, since this is our own natural environment, from living systems to society. But do we necessarily need complicated equations to understand diversity in the Nature? For some motions like chaos, simple equations have been identified, such as the 1D logistic (quadratic) map or the 3D Lorenz system, from which complex dynamical mechanisms, among which is chaos, have been clearly identified and understood.

Beyond the inspiring achievements in nonlinear dynamics theory, one of the nowadays hot research topics aimed at understanding complex motions and systems, is related to deterministic organisation of networks of oscillators in both finite- and infinite-dimensional situation. Within this topic, a particular phenomenon discovered in the early 2000, have attracted a strongly growing attention, namely *Chimera state*. Such solutions have been

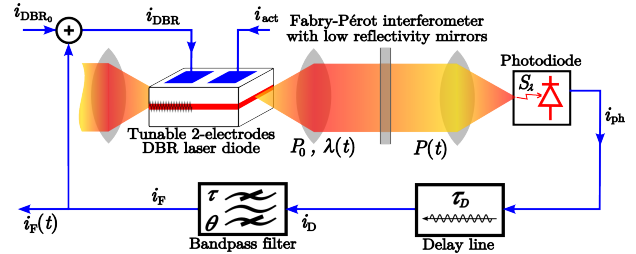


FIG. 1. Tunable semiconductor laser setup allowing for highly controllable multiple head Chimera states.

defined as the emergence of “incongruent” patterns of co-existing synchronous and incoherent behaviours, where different groups of oscillators within the network are exhibiting motions that are similar within a cluster, but “incongruent” between clusters. Discovered in 2002 by Kuramoto and Battogtokh [1], Chimeras states [2] have been experimentally observed in 2012 only, on spatio-temporal dynamics in the transverse plane of a light beam [3], and independently in the volume of a chemical reaction [4] and soon after, in mechanical experiments with coupled metronomes [5, 6]. Recently, Chimera motions were revealed in an even simpler system, however known for its infinite dimensional phase space, a nonlinear electronic delayed self feedback oscillator [7]. Exploring further this unexpected feature for the class of delay dynamics, we have specially designed a laser-based setup in which a complex organization of many multistable Chimera states can be obtained and described in a detailed way. Most importantly, thanks to the high control accuracy of the optoelectronic setup, novel Chimera features have been identified experimentally, and have been found in excellent qualitative agreement with numerical simulations, which will potentially open new fundamental as well as applied perspectives for Chimera states.

The article is organized as follows. We will first detail the structural and mathematical requirements of a de-

lay dynamical system in order to obtain Chimera, which requirements have closely guided the design of the experiment based on a tunable laser diode. The laser setup will then be presented in section II. Section III will report on the discovery of Chimera order cascade in a 2D-parameter space (spatio-temporal coupling parameters), as well as on the transition to turbulent-like behaviour when moving along a third parameter (feedback gain). The conclusion will propose to extend implications of our findings with delay systems onto other fields concerned by complex nonlinear dynamics, such as photonic brain-inspired computing and turbulent-laminar processes in fluid mechanics.

I. DELAY DYNAMICS REQUIREMENTS FOR CHIMERA

A delay differential equation (DDE) has the specificity to be a purely temporal dynamics, however having an infinite dimensional phase space [8–10] as for spatio-temporal dynamics modeled by partial differential equations. The common scalar form of such a DDE is often given by an equation $\varepsilon \dot{x}(s) = -x(s) + f[x(s-1)]$, where s is the time variable normalized to the delay, and f represents a nonlinear transformation of the amplitude variable x . Though being scalar and of a first order only, the initial conditions required to uniquely define a solution, take the form of a functional of time defined over a time delay interval i.e. $x_0(s)$ s.t. $s \in [-1; 0]$. In the case of a large physical delay, which implies $\varepsilon \ll 1$, the strong multiple time scale character allows for high complexity phase space [11], and spatio-temporal analogy have been proposed already more than 20 years ago [12] to help understanding the underlying system behaviour. The simple idea behind such space-time analogy is to represent the dynamics as the evolution with the discrete time n of the functional trajectory $\{x_n(\sigma) = x(s) | s = \sigma + n\eta, \text{ with } \sigma \in [0; \eta] \text{ and } n \in \mathbb{N}\}$. This results in a 1-Dimensional “spatial” distribution of continuously coupled amplitudes, over a finite “virtual space” interval $([0; \eta])$, with $\eta = 1 + \gamma$ and $\gamma = O(\varepsilon)$. The dynamics of this functional trajectory appear as a discrete iteration from n to $(n+1)$ according to a time step η close to unity (i.e. the delay). Space refers thus to the fast time scale $\sigma \in [0; \eta]$ (spatial “granularity” being of the order of ε), whereas discrete time variable n refers to the long time scale counting roughly the number of time delays.

In delay systems, Chimera is thus expected to appear as a rich multi-clustered pattern $x_n(s)$, self-sustained as n is growing. However, in its simplest scalar form a DDE does not allow for such (nearly) one-delay periodic patterns as they are Lyapunov unstable at any $\varepsilon > 0$ [13], all the space being rapidly filled by a unipolar amplitude [14]. We recently showed [7] that introducing a slow integral term to the DDE allows for the stabilization of such

patterns, giving rise to robust Chimera:

$$\varepsilon \frac{dx}{ds}(s) + x(s) + \delta \int_{s_0}^s x(\xi) d\xi = f[x(s-1)]. \quad (1)$$

Additional requirement for obtaining Chimera concerns the function f , which associated map ($x_{n+1} = f[x_n]$) has to exhibit multi-stability through a positive feedback at the zero unstable operating point, connecting two asymmetric extrema (a broad minimum for $x < 0$ leading to a stable equilibrium, and a sharp maximum for $x > 0$ leading to an unstable fixed point and chaos around it). Rewriting the integro-differential delay equation into a more common form, one obtains the following two coupled first order delay equation:

$$\begin{aligned} \varepsilon x' &= -\delta y - x + f[x(s-1)], \\ y' &= x, \end{aligned} \quad (2)$$

where the additional slow variable y accounts for the added integral term which weight is controlled by the additional parameter $\delta > 0$. This formulation allows to get a qualitative but effective analysis of the dynamics in terms of simplified slow-fast two-dimensional dynamics [7, 15], it however does not remove the difficulty to interpret detailed microscopic nature of the spatio-temporal phenomenon. Another formulation of such dynamics, more inspired by signal theory, involves a simple convolution product with the so-called filter impulse response $h(s)$, $x(s) = \int h(s-\xi) f[x(\xi-1)] d\xi$. $h(s)$ is originating from the linear left hand side of Eq.(1), its Fourier transform being simply the corresponding linear Fourier frequency filtering function. The nonlinear delay dynamics is thus revealed as a feedback loop oscillator as in Fig.1, in which a linear filter provides the argument x for the nonlinear function f , which output is delayed and serves then as the filter input. This “convolution product” allows for a straightforward space-time analogy, since rewriting it in order to reveal the discrete functional trajectory $x_n(\sigma)$, one obtains (see Supplementary Material):

$$x_n(\sigma) = x_{n-1}(\sigma) + \int_{\sigma-1}^{\sigma+\gamma} h(\sigma+\gamma-\xi) \cdot f[x_{n-1}(\xi)] d\xi, \quad (3)$$

which shows the mapping dynamics from x_{n-1} to x_n , via a spatial nonlinear and non-local coupling between the position σ and a ξ -shift around it, with $\xi \in [\sigma-\Delta; \sigma+\gamma]$. Equation (3) thus reveals f as the nonlinear coupling function, h as the coupling weight, and the quantity $(\Delta + \gamma)$ is an effective spatial range for the coupling, which spread is practically determined by the width of the impulse response h (see Supplementary Material).

II. LASER WAVELENGTH DELAY DYNAMICS

The photonic setup is depicted in Fig.1. It is designed according to the above described requirements allowing for the observation of Chimera in a delay dynamics. The

physics and photonic concepts are inspired by a wavelength chaos generator designed previously for optical chaos communication, where chaos was obtained from an Ikeda dynamics (given by DDE with a symmetric nonlinear function $f[x] = \beta \sin^2(x + \Phi_0)$ [16]). Two essential modifications are allowing for Chimera: (i) a bandpass filter instead of low pass one is providing the left hand side in Eq.(1), and (ii) a Fabry-Pérot (FP) interferometer instead of a birefringent one which is providing the asymmetric nonlinear Airy function:

$$f[x] = \frac{\beta}{1 + m \sin^2(x + \Phi_0)}. \quad (4)$$

The oscillating principles of such an optoelectronic tunable laser delay oscillator are as follow. A dual electrode tunable distributed Bragg reflector (DBR) laser diode emitting at $1.5 \mu\text{m}$ provides a laser beam, which wavelength deviation (corresponding to variable x) is proportional to a tuning electrode current i_{DBR} (another conventional active electrode receives the injection current i_{act} setting the emitted optical power). An offset current i_{DBR_0} is added to the tuning electrode for the central laser wavelength, thus allowing for the setting of the appropriate parameter Φ_0 in Eq.(4) (needed for the positive feedback condition). Wavelength fluctuations are then non linearly converted into intensity ones through the FP, as x is scanning back and forth the Airy function from the flat destructive interference condition up to the sharp constructive one. A photodiode is used to convert the optical intensity fluctuations into an electrical signal, which is then delayed in time by τ_D thanks to an easily tunable electronic delay line. This electronic path allows for an accurate control of the equation of motion (1), through an appropriate bandpass filter having characteristic times θ and τ defining the low and high cut-off frequencies of the filter respectively. The signal is finally amplified (setting the normalized gain β in Eq.(4)), before being fed back (i_F) onto the laser DBR tuning electrode. The electronic filter output i_F is the monitored time trace proportional to $x(s)$, from which space-time Chimera patterns $\{x_n(\sigma) | \sigma \in [0; \eta], n \in \mathbb{N}\}$ can be extracted and analyzed depending on the system parameters. The most important normalized parameters are the small quantities $\varepsilon = \tau/\tau_D$ and $\delta = \tau_D/\theta$ introduced in Eq.(1). These two quantities are practically influencing the actual shape and “spatial” spread of the impulse response h , $(\gamma + \Delta) \simeq \varepsilon \ln(\varepsilon\delta)^{-1}$, as discussed for Eq.(3) for the analogy of a weighting function in a network of non-locally coupled oscillators.

III. CASCADE OF MULTI-HEADED CHIMERA

As reported in [7], Chimera in DDE is revealed as the spontaneous emergence of a particular functional pattern $x_n(\sigma)$ showing sub-intervals over $[0; \eta]$ each of which being characterized whether by a nearly constant negative

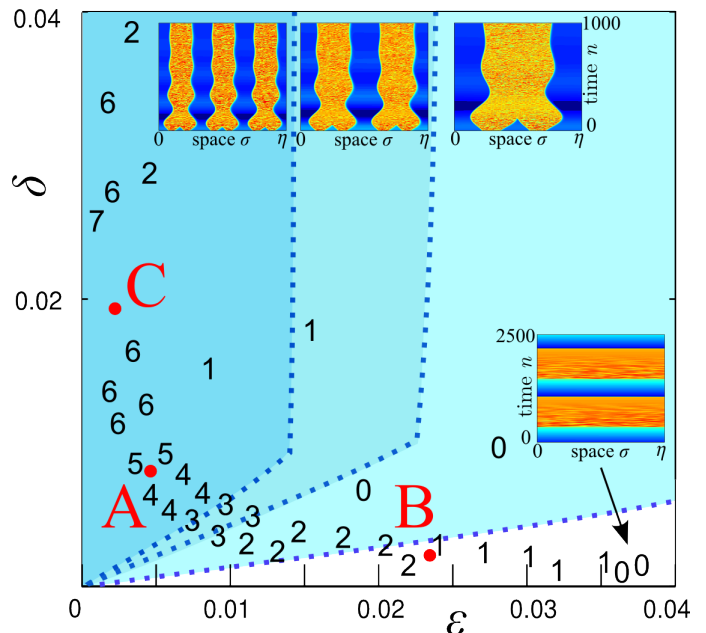


FIG. 2. (a) Observed numerical (colorized) and experimental (integer N) solutions in the parameter plane (ε, δ) , with $\beta = 2.0$ and $\Phi_0 = -0.4$. $N = 0$ or white region stands for chaotic breather [17], and otherwise one has N -headed chimeras. Crossing a dotted line (numerically determined) from the up-left to the low-right means a unit decrement for the maximal number N of observable chimera heads (any N_σ heads with $N_\sigma \leq N$ being possible). Insets are example of space-time plots for $N = 1, 2, 3$ (Chimeras) and 0 (chaotic breather).

amplitude, or by a chaotic-like oscillations (see space-time patterns in the in-box of Fig.2, and time traces in Fig.3). An amazing peculiarity is that such rich and organized functional behaviour in σ can be self sustained as n is iterated. When N_σ chaotic intervals of this kind exist for $\sigma \in [0; \eta]$, the Chimera is referred as to a N_σ -headed Chimera state.

Through the experimental behavior observed from the laser setup in Fig.1, as well as from the respective numerical simulations of its established model in Eq.(2), the (ε, δ) -parameter space is discovered to contain a specific multistable bifurcation structure. This structure reveals cascaded regions from the low-right to the up-left of the (ε, δ) -plane, which are successively embedded one in the other with increasing maximal integer N of any $N_\sigma \leq N$ number of possible Chimera heads. As shown in Fig.2, these regions are delimited by bifurcation curves characterized by the transition from N to $(N - 1)$ as ε is increased, and δ is decreased. These regions accumulate with increasing N close to the $\varepsilon = 0^+$ -axis. On the opposite side, the lowest value $N = 0$ finishes on the $\delta = 0^+$ -axis. This region does not lead any stable Chimera motion, but reveals so-called *chaotic breather* solutions [17], a slow envelope alternating fast chaotic oscillations and slow drifts, over time durations of the order of δ^{-1} . Typ-

ical Chimera patterns and chaotic breather dynamics are shown in insets of Fig. 2. Numerics (full scan) and experiments (for which a few points only are explored while decreasing τ_D to scan a hyperbola defined by $\varepsilon\delta = \text{constant}$) reveal excellent qualitative agreement in the observation of this unusual bifurcation structure. Quantitative discrepancies between numerics and experiments are noticed for the absolute position of the N -transition lines, probably related to the influence of noise as well as to uncertain calibration of experimental parameters.

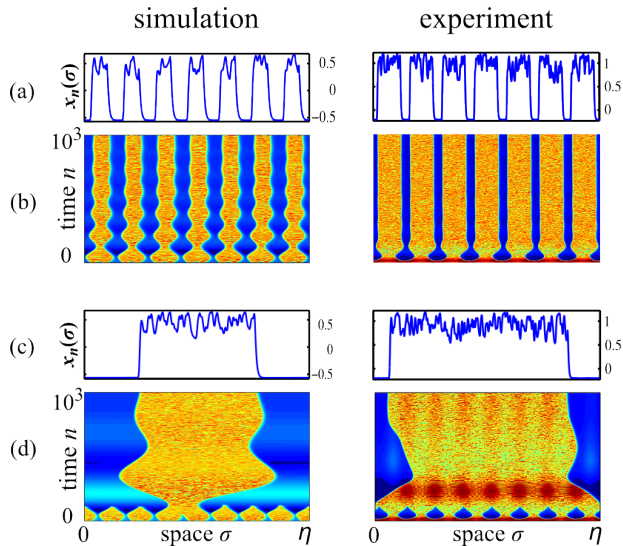


FIG. 3. Examples of emergence and stabilization of N_σ -headed Chimera at point C in Fig.2 ($N_\sigma = 7$ and 1 for (a,b) and (c,d) respectively). Left panel: Numerics; Right panel: Experiment. (a,c): asymptotic (biggest n) functional trajectory $x_n(\sigma)$. (b,d) spatio-temporal pattern birth of N_σ -headed Chimera. (b): 7-periodic small initial forcing; (d): same as (b) but with 8-periodic small initial forcing; $N_\sigma = 8$ is not stable, thus leading to a single-headed asymptotic chimera state.

Figure 3 illustrates how a maximum number N_σ is experienced, both in numerics and experiments: for a fixed parameter setting (ε, δ) (point C in Fig.2) corresponding to $N = 7$, one observes that an initial condition imposed as a small sine modulation with 7 periods within η , indeed leads to the birth of a 7-headed Chimera. Trying a small sine modulation with 8 periods results in spontaneous switch to the birth of a lower number of heads, e.g. $N_\sigma = 1$ in the presented case (but any other $N_\sigma \leq N = 7$ can be observed in principle, even chaotic breather, depending on initial conditions). Looking more carefully at the numerical bifurcation lines in Fig.2, one notices their threshold-like shape, with a nearly horizontal proportional part close to the origin, and then an almost vertical part after some threshold. We anticipate that this peculiar double shape of the bifurcation curves is related to different bifurcation scenarios for the destabilization of the N -headed Chimera states. Typical N to $(N - 1)$ bifurcation events occur-

ring while crossing such curves, are illustrated in Fig.4, with captured space-time snapshots for 2-to-1 and 6-to-5 heads transitions. Again, excellent qualitative agreement is found between experiments and numerics. More detailed analysis of this novel phenomenon is left to a later report.

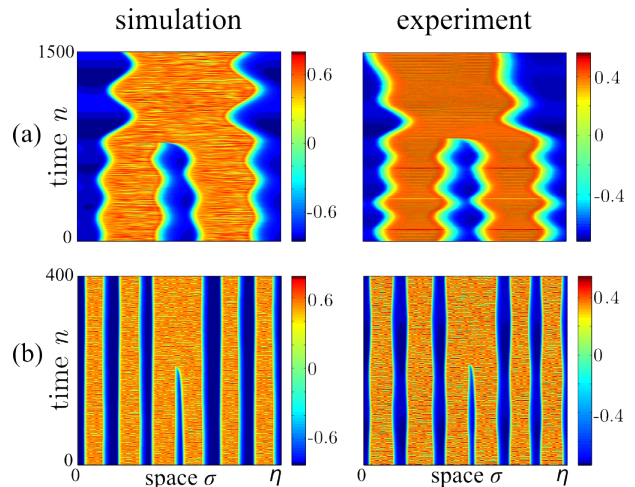


FIG. 4. Typical bifurcation events as N -headed Chimera becomes unstable, being replaced by $(N - 1)$ heads. (a): 2-to-1 transition (point B in Fig.2). (b): 6-to-5 transition (point A in Fig.2).

Figure 2(a) reveals that model (1) is highly multi-stable for small and intermediate ε . This suggests to explore the basins of attraction of the different co-existing attractors. Since time-delayed systems are infinite dimensional through their initial conditions being functional $\{x_0(s) | s \in [0, 1]\}$, a precise topological characterization of the basins structure is not directly possible. One can however try to estimate the relative size (measure) of the basins in terms of occurrence probability for each possible solution, after re-setting many different random initial conditions. This is illustrated in Fig.5, which shows the evolution vs. ε of the probability occurrence for N_σ -headed Chimera for 3 fixed δ -values, with $N_\sigma = 0$ to 5 (0 corresponding to chaotic breather). Each probability has been calculated with 300 different initial noisy conditions $x_0(s)$ (uniform amplitude distribution of $x \in [-1; 1]$). In Fig.5(a) ($\delta = 0.02$), for small ε the most probable solutions are high order multi-headed Chimera, a small fraction only of initial conditions leading to one- or two-headed Chimeras. As ε is increased, $N_\sigma = 1$ and $N_\sigma = 2$ basins are revealing higher and higher occupation of phase space. For an intermediate range of ε , one notices that two-headed Chimera basins reaches a maximum, prevailing on the other possible N_σ with approximately 60% of probability of occurrence around $\varepsilon = 0.005$. For larger values of ε , one-headed Chimera basin appears to occupy almost the full explored phase space. In Fig. 5(b) and (c) corresponding to smaller

δ -values, qualitatively similar features are observed, except that higher-order Chimeras are less and less probable (they would require smaller ε), and lower N_σ orders predominate together with a growing influence of the chaotic breather (black) as it is visible already in Fig.2(a) from the positions of the bifurcation curves.

Based on these numerical simulations, we summarize that multi-headed Chimeras represent an essential part of the solutions exhibited by Eq.(2), higher order Chimeras requiring small ε to predominate.

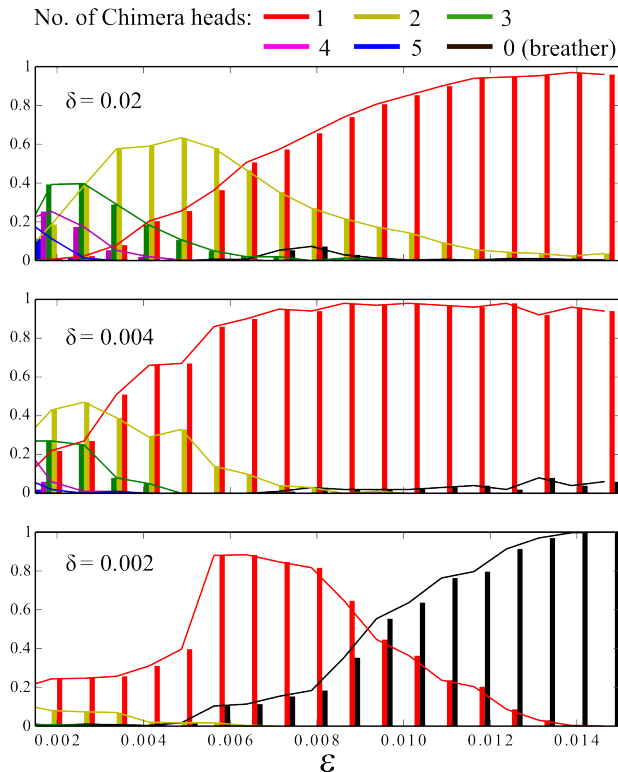


FIG. 5. Probability of occurrence under random initial conditions, for Chimeras with different number of heads, and for three different values of δ (horizontal cut in Fig.2).

The bifurcation diagram (Fig. 2) is obtained for a fixed normalized gain $\beta = 2.0$, providing Chimera states as alternated chaotic and quite amplitudes. Increasing β progressively destroys the previously sustained Chimera patterns as n is iterated. Greater β -values indeed gives rise to a spatio-temporal turbulent-like intermittent behaviour, including both chaotic and quite amplitudes in an irregular non-sustained fashion. This situation is illustrated in Fig.6 with space-time plots for 2 higher values of β . This transition to turbulence is again nicely consistent between numerics and experiments. On the contrary, smaller values of β transforms progressively the chaotic heads into more regular (periodic) or even quite plateaus, which situation could have been recently analytically explored [15, 18].

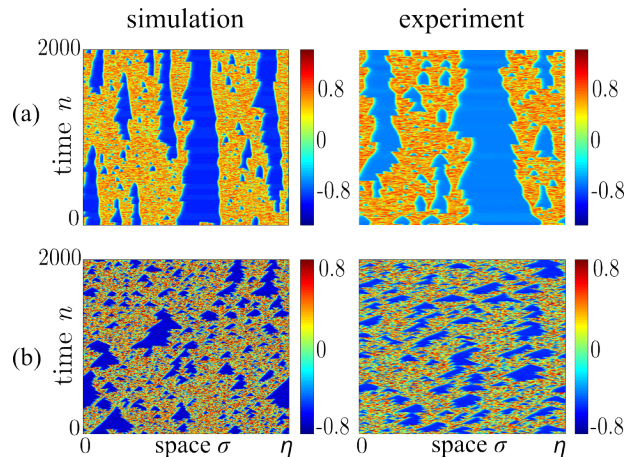


FIG. 6. Progressive route to turbulence as β ($\Phi_0 = -0.4$, at point A in the (ε, δ) -plane of Fig.2) is increased, revealing more and more irregularly vanishing and appearing number of Chimera heads N_σ as time n is running. (a): $\beta = 2.4$. (b): $\beta = 4.0$.

IV. CONCLUSIONS

Delay equations have always raised difficult and complex issues, e.g. motivated whether by technological contexts such as remote satellite control at the beginning of space exploration, or by the understanding of complex motion observed in blood cell production disorders [8], or even through the quest for optical chaos [9]. Beyond theoretical interests, they even led to surprising experimental success, e.g. high spectral purity microwave optoelectronic oscillator for improved Radar performances [19], or demonstration of optical chaos communications for physical layer encryption in fiber networks [20–22], or even more recently with the demonstration of novel brain-inspired computing concepts[23] in photonic[24]. In the present letter we have reported on a yet unexplored potential of delay systems in terms of their self-organization capability through a virtual space-time analogy of delay equations, allowing for the interpretation of these complex self-organized motions in terms of Chimera states. The reported excellent agreement between numerical simulations of a generic model, and the observed phenomena in a laser-based experiment, suggests the robustness and the intrinsic character of the underlying dynamical concepts. We anticipate that such delay systems and their related dynamical phenomena will represent a simple but efficient theoretical tools for investigation of complex self-organized motions, as they are naturally developed in living systems, pattern formation, fluid dynamics phenomena, as well as behavior in social and technological networks.

This work was supported by the European project PHOCUS (FP7 grant 240763), and the Labex ACTION program (contract ANR-11-LABX-01-01). BP and YM acknowledge the support of the Region Franche-Comté.

METHODS

Experiments: The acquired signal is corresponding in the setup of Fig. 1, to the output of the bandpass filter limiting the dynamics in the feedback loop. This signal corresponds mathematically to the normalized variable $x(t)$ in Eqs. (1)-(3), and it is physically proportional to the laser wavelength deviation. As described in the setup section, an offset current applied to the DBR tuning electrode of the laser allowed to adjust the normalized parameter Φ_0 , thus allowing the selection of the delayed dynamics operation along a positive slope of the Fabry-Pérot Airy function. Chimera pattern can then be obtained by increasing gradually from zero the feedback loop gain of the dynamics, which gain is electronically and linearly adjustable via a DC voltage applied to an analogue electronic multiplier.

A large memory depth (up to 32 million points) digital Lecroy oscilloscope is used for real-time acquisition of long time traces covering up to 10000 time delays. This oscilloscope also provides specific time trace processing capability through short Matlab routines, thus enabling the real-time visualization of the space-time patterns shown in Figs. 2, 3, 4 and 6. The main difficulty for this custom real time Chimera pattern observation, was to design the adequate algorithm capable for the accurate (10^{-5} required precision) and fast extraction of the spatial width $\eta = 1 + \gamma$, for which only the Chimera can be clearly observed as a vertical pattern over thousands of time delay duration. This pattern is whether strongly tilted in the space-time plane at 10^{-4} precision, or even completely invisible for worth precision. The algorithm aims at detecting the most frequent time difference between two plateau-to-chaos sharp transitions in the waveform. Chimera pattern evolution were then analyzed while scanning the (ε, δ) -plane, which scanning is performed along hyperbola corresponding to constant characteristic times of the bandpass filter τ and θ (hyperbola equation defined as $\varepsilon\delta = \tau/\theta = \text{constant}$). The hyperbola scan is obtained through the easy electronic tuning of the time delay τ_D via the increase of a TTL clock frequency f_{CLK} . This clock indeed controls the speed at which the digitized signal is traveling through the FIFO memory depth used in our digital delay line, the time delay reads then: $\tau_D = N_0/f_{\text{CLK}}$ (where N_0 is a constant integer related to the memory depth of 4096, and to the small number of sampling periods required by

the Analog-to-Digital conversion used in the delay line). Increasing f_{CLK} remains to scan the hyperbola from the top left to the down right, i.e. for decreasing maximum number of Chimera heads (the highest possible number being forced by adequate initial conditions, on the top left of the hyperbola). Different hyperbola were scanned through the choice of different θ (i.e. different high pass cut-off frequencies). The observed Chimera pattern in the graphical Matlab window of the oscilloscope allowed for the easy detection of the number of heads N_σ , or of the chaotic breather solution (0-head), which number can then reported in Fig. 2.

Numerics: Fourth order Runge-Kutta integration scheme is used for all the numerical experiments to calculate $x(t)$, with a fixed time step $h = \varepsilon/10$. The space-time plots are obtained as in the experiment, through the determination of the duration η revealing “in average” vertical patterns, stacking vertically the n_0 successive waveforms $\{x(t) = x_n(\sigma) | t = (n\eta + \sigma)\tau_D\}$ with $\sigma \in [0, \eta], n = 1, 2, \dots, n_0\}$.

The procedure for calculating the bifurcation diagram (Fig. 2) is the following. Bifurcation events are detected for several vertical lines in the (ε, δ) -plane (constant ε). For progressively decreasing δ , the sustained maximum N -headed Chimera is tested through the calculation of the dynamics over 10^5 time delay durations, the solution being initially forced (imposing $x(t)$ for $t \in [-\tau_D; 0]$) with a N -periods sinusoid. Each δ -value at which N can not be sustained whereas $N - 1$ can, is used to obtain one point of the N to $N - 1$ bifurcation curve.

Each chimera basin diagram (Fig. 5) is calculated for 18 values of ε . The initial interval of $[-\eta; 0]$ is interpolated from random initial conditions uniformly distributed within range $[-1; 1]$. For each ε , 300 numerical experiments is conducted, thus allowing to establish a histogram for the 300 different asymptotic chimera patterns calculated after 10^5 time delay evolution.

AUTHORS' CONTRIBUTION

LL designed the experiment, performed the measurements, provided the theoretical dynamics modeling, developed its coupled-network interpretation, contributed to the analysis, and participated to the writing. BP performed the numerical simulations and participated to the experimental record and the writing. YM supervised the Chimera analysis, provided theoretical interpretations for the observed phenomena and participated to the writing.

-
- [1] Y. Kuramoto and D. Battogtokh, Nonlinear phenomena in complex systems **5**, 380 (December 2002)
 [2] D. M. Abrams and S. H. Strogatz, Phys. Rev. Lett. **93**, 174102 (October 2004)
 [3] A. M. Hagerstrom, T. E. Murphy, R. Roy, P. Hövel, I. Omelchenko, and E. Schöll, Nature Physics (London)

- 8**, 658 (September 2012)
 [4] M. Tinsley, S. Nkomo, and K. Showalter, Nature Physics (London) **8**, 662 (2012)
 [5] E. A. Martens, S. Thutupalli, A. Fourrière, and O. Halatschek, Proc. Nat. Acad. Sci. **110**, 10563 (June 2013)

- [6] T. Kapitaniak, P. Kuzma, J. Wojewoda, K. Czolczynski, and Y. Maistrenko, *Scient. Rep.* **4**, 6379 (September 2014)
- [7] L. Larger, B. Penkovskiy, and Y. L. Maistrenko, *Phys. Rev. Lett.* **111**, 054103 (August 2013)
- [8] M. Mackey and L. Glass, *Science* **197**, 287 (1977)
- [9] K. Ikeda, *Optics Commun.* **30**, 257 (August 1979)
- [10] S. Chow and J. K. Hale, “Dynamics of infinite dimensional systems,” (Springer-Verlag, 1987)
- [11] M. Le Berre, E. Ressayre, A. Tallet, and Y. Pomeau, *Phys. Rev. A* **41**, 6635 (June 1990)
- [12] F. T. Arecchi, G. Giacomelli, A. Lapucci, and R. Meucci, *Phys. Rev. A* **45**, R4225 (April 1992)
- [13] A. Sharkovsky, Y. Maistrenko, and E. Romanenko, “Difference equations and their applications,” (Kluwer Acad. Publ. (Naukova Dumka, Kiev, in Russian, 1986), 1993) Chap. 3
- [14] G. Giacomelli, F. Marino, M. A. Zaks, and S. Yanchuk, *Europhys. Lett.* **99**, 58005 (September 2012)
- [15] L. Weicker, T. Erneux, O. D’Huys, J. Danckaert, M. Jacquot, Y. Chembo, and L. Larger, *Phyl. Trans. Roy. Soc. A* **371**, 20120459 (2013)
- [16] L. Larger, J.-P. Goedgebuer, and J.-M. Merolla, *IEEE J. Quantum Electron.* **34**, 594 (April 1998)
- [17] Y. C. Kouomou, P. Colet, L. Larger, and N. Gastaud, *Phys. Rev. Lett.* **95**, 203903 (November 2005)
- [18] L. Weicker, T. Erneux, O. d’Huys, J. Danckaert, M. Jacquot, Y. Chembo, and L. Larger, *Phys. Rev. E* **86**, 055201(R) (November 2012)
- [19] X. S. Yao and L. Maleki, *Electron. Lett.* **30**, 1525 (September 1994)
- [20] G. D. VanWiggeren and R. Roy, *Science* **279**, 1198 (February 1998)
- [21] J.-P. Goedgebuer, L. Larger, and H. Porte, *Phys. Rev. Lett.* **80**, 2249 (June 1998)
- [22] A. Argyris, D. Syvridis, L. Larger, V. Annovazzi-Lodi, P. Colet, I. Fischer, J. Garcia-Ojalvo, C. R. Mirasso, L. Pesquera, and A. K. Shore, *Nature (London)* **438**, 343 (November 2005)
- [23] H. Jaeger and H. Haas, *Science* **304**, 78 (April 2004)
- [24] L. Larger, M. C. Soriano, D. Brunner, L. Appeltant, J. M. Gutierrez, L. Pesquera, C. R. Mirasso, and I. Fischer, *Opt. Express* **20**, 3241 (January 2012)